SEDIMENT BUDGET FOR SOURCE ANALYSIS:
LE SUEUR WATERSHED, MINNESOTA

Patrick Belmont, National Center for Earth-surface Dynamics, Assistant Professor, Watershed Sciences, Utah State University, 5210 Old Main Hill, Logan, Utah 84322, Tel: 435-797-3794, patrick.belmont@usu.edu; Enrica Viparelli, Postdoctoral Research Associate, National Center for Earth-surface Dynamics, University of Illinois, Urbana-Champaign, Ven Te Chow Hydrosystems Laboratory, 205 North Mathews Ave., Urbana, Illinois 61801; Peter R. Wilcock, National Center for Earth-surface Dynamics, Professor, Geography and Environmental Engineering, Johns Hopkins University, 3400 North Charles Street Baltimore, MD 21218

INTRODUCTION

Excessive suspended sediment in rivers is often the combined result of complex interactions between climate, hydrology, geomorphology, and human land use. Developing a process-based understanding of these interactions represents a formidable challenge for sustainable watershed management. Toward this end, sediment budgets and sediment routing models can be used in combination as effective tools for assembling various types of information regarding the sources, sinks, and transport pathways of fine-grained sediment in rivers. Here we discuss the development of a sediment budget and routing model for the Le Sueur River, south-central Minnesota, a watershed that is naturally inclined to generate a high sediment yields for reasons that are readily compounded by ongoing human activities.
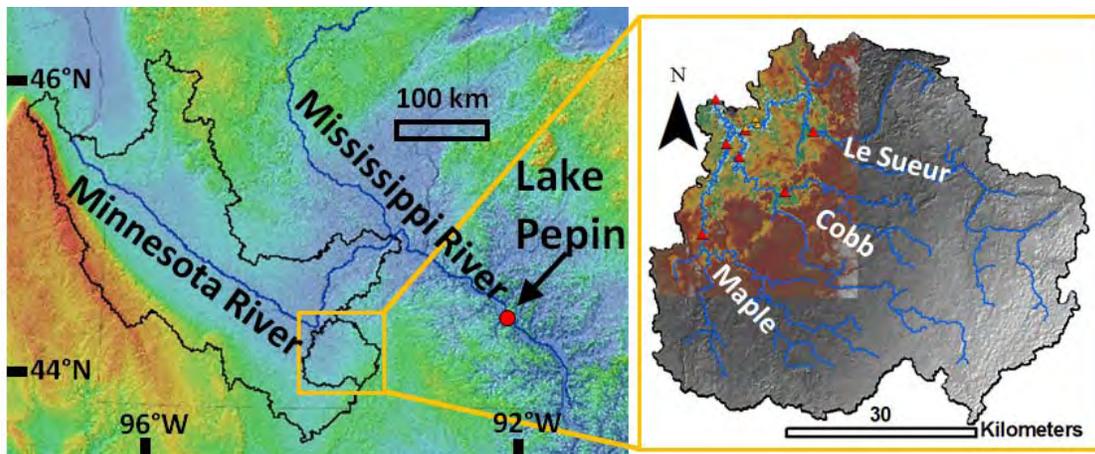

Figure 1 Location of the Le Sueur watershed, southern Minnesota. Triangles indicate the location of gaging stations on the main stems (red) and ravines (orange). The colored DEM shows the extent of lidar data.

The Le Sueur River watershed comprises 2,880 km^2 of the greater 43,400 km^2 Minnesota River watershed (Figure1). Multiple reaches of the Le Sueur and Minnesota rivers, as well as Lake Pepin, a naturally dammed lake on the Mississippi River downstream from the confluence with the Minnesota River, are impaired for excess fine sediment under Section 303d of the US Clean Water Act. The record of sedimentation in Lake Pepin indicates that sediment loads have

increased significantly since the onset of widespread row-crop agriculture in this region, beginning around 1830 (Engstrom et al., 2009). Trace element analyses indicate that as much as 85 – 90% of sediment deposited in Lake Pepin is derived from the Minnesota River watershed (Kelley and Nater, 2000), a trend that appears to be consistent prior to and throughout the tenfold increase in sedimentation rates observed over the past 180 years. Modern sediment gaging throughout the Minnesota River basin indicates that a disproportionate amount (~ 24 – 30%) of that fine-grained sediment originates from the Le Sueur River (MPCA et al., 2007).

The Le Sueur watershed has been profoundly modified by human activity, particularly agriculture, and so naturally the a priori assumption is made that human land use practices are primarily responsible for observed excessive suspended sediment loads. This assumption is not entirely unreasonable considering the extensive list of human modifications which includes wholesale drainage of previously extensive wetlands that comprised 15-35% of the watershed (Marschner, 1974; MDNR, 2007; Prince, 1997; Thompson, 2002), a dramatic increase in drainage density and extension of the fluvial network by excavation of agricultural ditches, which now comprise 25% of the fluvial network, conversion of native forest and long grass prairie vegetation to row crop agriculture covering more than 75% of the watershed area, a modest amount of urban development, mechanical tillage of the soil during late fall and spring, bare earth conditions during a hydrologically and geomorphically sensitive period in early spring, and an extensive (and expanding) network of artificial subsurface tile drainage, which, in places, contains surface inlets (Spaling and Smit, 1995; Blann et al., 2009). Management practices, such as conservation tillage, grass buffer strips surrounding ditches, protected riparian forest lining parts of the channel network, and a few restored prairie and wetland areas, have been designed to minimize sediment erosion, but no comprehensive watershed management strategy has been developed and the effectiveness of these practices, individually or collectively, is not well understood. Also, Gran et al. (2009) recognize that the natural geomorphic context of this landscape has established conditions that are conducive to rapid landscape evolution, high rates of sediment transport, and perhaps most importantly, enhanced sensitivity to changes in hydrology, climate, and vegetation, as discussed above.

The two main factors that have naturally primed the Le Sueur watershed for high sediment loads are the easily erodible substrate and a nearly instantaneous baselevel fall that occurred approximately 11,500 radiocarbon years before present (rcybp). The substrate is composed of fine-grained till interbedded with glaciofluvial sand deposits. The western 2/3 of the basin are mantled with a relatively thin (tens of cm to a few m) glaciolacustrine deposit from Glacial Lake Minnesota. Around 11,500 rcybp Glacial Lake Agassiz catastrophically drained through the Minnesota River valley, one of several such events, resulting in vertical incision of up to 70 meters (Clayton and Moran, 1982; Matsch, 1983). This incision imparted a drop in baselevel for tributaries of the Minnesota River. The resulting knickpoint that formed in the Le Sueur has migrated approximately 35 km up all three branches of the river network, including the main stem and two main tributaries, the Cobb and Maple rivers (Figure 2). The record of incision and knickpoint propagation is well recorded in a flight of terraces. In the wake of the knickpoint, tall bluffs are formed adjacent to the river and steep first- and second-order tributaries, or ravines, have developed to connect the relatively flat uplands with the incised river valley.
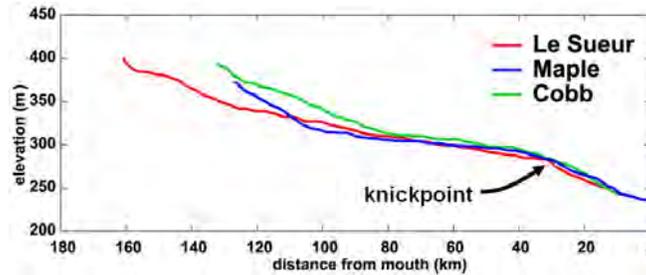
Figure 2 Longitudinal profiles for the Le Sueur, Cobb, and Maple Rivers. We interpret the anomaly in local channel slope relative to contributing drainage area as the uppermost extent of incision that has resulted from baselevel fall 11,500 rcybp.

Climate has also been systematically changing over the past several decades in this region. Temperatures are generally rising, resulting in warmer winters, higher minimum air temperatures, and rising ground temperatures that have been recorded at more than 10 m depth (Baker and Baker, 2002). Ice-out dates are generally occurring earlier in the spring, ice-in dates are typically occurring later in the year, the date of first spring runoff is occurring earlier (at a rate of 0.3 days/year) over the period between 1964 and 2000 (Johnson and Stefan, 2006) and stream temperatures throughout the year have been documented to be rising. General increases in precipitation have been documented by Changnon and Kunkel (1995), and increased number of rain days and increased frequency of heavy rain events were documented by Kunkel (1999). Novotny and Stefan (2007) found strong correlations between increases in precipitation and multiple metrics of stream flow throughout southern Minnesota, but note that the increases in stream flow are likely caused by a combination of changes in both climate and land use.

It is in the context of this rapidly evolving landscape that has been profoundly altered by human activity over the past 180 years, and is currently subject to a changing climate, that we have developed an integrated sediment budget and sediment routing model in an attempt to synthesize all available information about sediment sources, sinks, and transport pathways, and ultimately make predictions about how future watershed management alternatives might impact water quality and sediment dynamics. A sediment budget provides the basis for assembling all of the various lines of evidence we have compiled with respect to the rates of erosion and deposition throughout the watershed, including water and sediment gaging data at a number of sites throughout the watershed (Figure 1), morphometric analyses from high resolution (1 m gridded) aerial lidar topographic data, annual differencing analysis of ultra-high resolution (0.5 - 2 cm) ground-based lidar measurements of annual bluff erosion, aerial photo analysis of decadal river meander migration rates, bluff retreat rates, rates of ravine elongation, and geochemical fingerprinting using meteoric Beryllium-10 (^{10}Be). The one-dimensional sediment routing model provides the numerical framework to develop predictions and hypotheses about transport and storage of sediment within the system. Specifically, it allows us to make predictions regarding the production, transport, and storage of sediment and tracers in the channel and floodplain, the morphodynamic responses to changes in the magnitude and distribution of sediment sources, and the rate of sand and mud transport through the system, which will inform our understanding of the time lag that could be expected between implementation of mitigation strategies and resulting improvements in water quality.

METHODS

Our sediment budget considers inputs from four primary sources, the broad and relatively flat uplands, which are dominated by agriculture, tall bluffs, which are composed of interbedded fine-grained till and glaciofluvial sand, and some of which are capped by 2-3 m thick strath terrace alluvial deposits, steep first- and second-order tributaries, which we call ravines, and channel banks, which we define as channel boundary features shorter than 3 m, as represented on the aerial lidar, to distinguish them from bluffs. Flows were continuously monitored by the US Geological Survey and Minnesota Pollution Control Agency (MPCA) at several gaging stations distributed above and below the knickpoint, throughout the watershed (Figure 1). Approximately 30-40 surface grab samples were collected and processed by the MPCA throughout each year of record, focused primarily on storm events. Samples were analyzed for TSS and converted to flow-weighted mean sediment concentrations by MPCA using the US Army Corps of Engineers FLUX program.

Topographic analyses were conducted using a 30 m digital elevation model (DEM) obtained from http://seamless.usgs.gov, as well as a 1 m gridded lidar DEM that covered approximately 1/3 of the basin, including the entire knickzone, obtained from Blue Earth County, Minnesota. Computation of contributing drainage area, extraction of the channel network, slope-area analysis, and measurement of local relief were all conducted using the 30 m dataset in ArcGIS (ESRI, Redlands, CA). Slope-area analysis to identify the location of knickpoints in the system was conducted using the Stream Profiler Utility (geomorphtools.org) with a 3 m contour interval and 1 km smoothing window, and an empirically derived reference concavity of 0.45. Local relief was measured using the focal range algorithm in ArcGIS with a circular observational window that ranged in diameter from 100 – 5000 m. Ravines were manually digitized from the lidar DEM and a semi-transparent hillshade. Bluffs were extracted from the lidar using a semi-automated process that used neighborhood analysis in ArcGIS to identify areas that contained more than 3 meters of relief within an 81 m^2 moving observational window. The results of that algorithm were refined by removing areas within the delineated ravines. We then manually differentiated between bluffs that were directly connected versus disconnected from the river and only connected bluffs were used in the calculation of bluff sediment yields because field observations suggested that yields from disconnected bluffs are likely negligible.

A ground-based lidar survey was conducted by Day et al. (in prep, pers. comm.) in 2007, 2008, and 2009 using an Optek scanner (Optek Technology, Inc., Carrollton, TX) to directly measure annual bluff erosion rates. Point cloud data from scans were compiled, aligned, filtered to remove vegetation and erroneous points, and differenced in x, y, and z dimensions using PolyWorks software v. 10.1.14 (InnovMetric, Quebec, Canada). Results presented here are preliminary, but are not likely to change significantly based on comparison with two other bluff erosion datasets, one from physical surveys in the nearby Blue Earth River, and another from air photo analysis of bluff retreat between 1938 and 2005.

Analyses of aerial photographs were conducted to measure river meander migration rates, measure bluff retreat rates, and identify regions of ravine planform change between 1938 and 2005. The 1938 photos were manually scanned and georeferenced. Geo-referencing error was quantified by the root mean square method to be approximately ± 4 m over the entire study area.

However, the error associated with any given measurement varied slightly from photo to photo. To compute bluff retreat rates and mean annual erosion rates between 1938 and 2005, the crests of 80 bluffs were manually traced on both sets of photos. An upper bound on the volume of sediment eroded from bluffs was obtained by assuming parallel retreat of the crest and toe. A lower bound was obtained by assuming wedge retreat, such that the toe of the bluff was assumed to not have moved between 1938 and 2005. To compute bluff sediment loads in terms of mass, we multiply by the bulk density (1.8 Mg/m^3) and correct for the proportion that is composed of fine grained material that would likely be transported as washload (0.65).

We measured the migration distance of the river between 1938 and 2005 using the NCED Planform Statistics Tool (http://www.nced.umn.edu/content/tools-and-data) to estimate net erosion that has resulted from channel adjustment. Local net sediment contributions from streambanks were computed following Lauer and Parker, (2008) as:

$$V_{bank} = \sum_{i=1}^{i_{max}} M \cdot \Delta\eta \cdot \Delta l \qquad\qquad 1$$

where V_{bank} is the volume of sediment contributed from the banks on an annual basis, M is the migration rate (m yr^{-1}), $\Delta\eta$ is the difference in elevation between the depositing and eroding bank (m), and Δl is the spatial step (moving sequentially downstream) between computational nodes (i), 10 m in this case. To compute local, net bank sediment loads in terms of mass we multiply by the bulk density (1.3 Mg/m^3) and correct for the proportion that is composed of fine grained material that would likely be transported as washload (0.5). The elevations of the opposing banks were initially extracted from the lidar and then used to develop a synthetic relationship that generalizes the way in which $\Delta\eta$ varies in the downstream direction in both modeled reaches. Because hydrology dictates channel size, the method described above assumes that the average channel width and depth do not change as a result of channel migration. While this is often a reasonable assumption over multi-annual or decadal timescales, significant changes in the magnitude and/or frequency of high flows can result in channel widening, which also causes a net flux of sediment to the channel. The volume of sediment contributed from channel widening can be computed as:

$$V_{bank-w} = \Delta B_c \cdot h_0 \cdot \Delta l \qquad\qquad 2$$

In collaboration with the Water Resources Center at Minnesota State University, we established automated samplers to collect suspended sediment samples from two ravines during storm events in 2008. Annual loads were computed from measured TSS data and extrapolation to missing storms. The Hwy90 ravine was instrumented with two gages, one near the tip (UHwy90) and the other near the outlet to the Le Sueur (LHwy90). The Hwy8 ravine was instrumented with one sampler near the outlet to the Le Sueur. Azmera et al. (2009) developed a numerical model for ravine erosion following Torri and Borselli (2003), applying the Universal Soil Loss Equation (USLE) to estimate upland contributions to the ravine and using calibrated erosion rate equations to estimate sediment contributions from the ravine side walls and channel bed, as well as deposition within the ravine.

The 1D sediment and radionuclide routing model is embedded in an excel spreadsheet that will be freely downloadable from the NCED Stream Restoration Toolbox. Beyond what is presented

here, more details on the development and application of, and assumptions underlying, the model are presented in two manuscripts currently in preparation (Viparelli et al., *in prep A*; Viparelli et al., *in prep B*). Our routing model differs from other water quality models in several ways. Specifically, our model allows floodplains to morphologically evolve, thereby influencing hydraulics and the probability of future deposition; conserves tracers in the floodplain, and allows floodplains to act as a source or sink; focuses on average tracer concentration in deposited sediment at the reach scale, with the average computed over multiple hydrographs (i.e. years); and accounts for radionuclide production and decay in the floodplain and converges toward a long-term steady state. Synthetic relations for the routing model were developed from empirical data to compute total drainage area, upland drainage area, ravine area, channel width, floodplain width, and channel sinuosity at each computational node as a function of channel or valley coordinate. Synthetic relations were also developed to compute the fraction of sand and mud in the substrate, basal floodplain layer, and in the main floodplain, as a function of valley coordinate. The model keeps track of sand and mud tracers contributed from each of the sources and applies a mass balance approach to track geochemical tracers during transport in the channel and during channel-floodplain exchange processes.

General input parameters used for model runs on the Maple River are shown in Table 1. Setup parameters were specified based on approximate locations of field measured cross sections, with computational nodes every 1 km valley distance. Channel gradient was extracted from the lidar data, averaged over 600 meters centered on the cross section location. The longitudinal profile was extracted from the 30 m DEM. The incision rate is an estimate based on the apparent Holocene average rate. The Chezy friction coefficient for the channel is based on stage-discharge relationship at a USGS gage. Active layer thicknesses are averages based on field observations.

Table 1 Routing model input parameters.

Setup Parameters		Channel Parameters		Sediment Parameters	
multiple	Run duration	specified	Longitudinal profile	0.3	Characteristic diameter of sand fraction (mm)
7	Number of bins in flow duration curve	0.001	Incision or aggradation rate of lower reach (m/y)	0.03	Settling velocity of sand (m/s)
variable	Number of time steps each year	0.0059	Chezy channel friction coefficient	0.008	Settling velocity of mud (m/s)
50	Valley length of upper reach	0.01	Chezy floodplain friction coefficient	2.6	Sediment density (g/cm^3)
30	Valley length of lower reach	0.4	Active layer thickness in the upper reach	0.05	Floodplain trapping efficiency for sand
1000	Downvalley step length (m)	0.3	Active layer thickness in the lower reach	0.4	Fraction of sand transferred from load to point bar
		0.4	Channel bed porosity	0.3	Fraction of mud transferred from load to point bar
				551	Sand feed rate at upper end of study reach (Mg/yr)

RESULTS

The spatial extents of the four primary sediment sources are shown in Table 2, organized by their location relative to gaging stations with the lower gage of the Le Sueur tributary located immediately upstream from the confluence with the Cobb River (see Figure 1). The Le Sueur watershed includes all three tributaries, plus the area between the lower gages on the tributaries and the watershed mouth. Uplands, including field and non-field, comprise the vast majority of the watershed area. The majority of bluff area is found within the knickzone, below the upper gages. In the Le Sueur tributary, three percent of the bluffs are located above the upper gage and 97% located between the gages. In the Maple and Cobb watersheds, delineated at the lower gages, 23% and 25% of bluff area is located above the upper gage, respectively, with the

remainder located between the gages. A similar trend is observed for ravines, with little to no ravine area located above the upper gages.

Table 2 Spatial extent of sediment sources with respect to gaging stations.

	Le Sueur Tributary			Maple River			Cobb River			Le Sueur Watershed		
	Above upper gage	Between gages	Sum at lower gage	Above upper gage	Between gages	Sum at lower gage	Above upper gage	Between gages	Sum at lower gage	At tributary gages	Between tributary gages and mouth	At mouth
Total (m²)	9.03E+08	2.39E+08	1.14E+09	8.00E+08	8.44E+07	8.84E+08	3.34E+08	4.53E+08	7.87E+08	2.81E+09	6.36E+07	2.88E+09
Upland (m²)	9.03E+08	2.37E+08	1.14E+09	7.99E+08	8.26E+07	8.82E+08	3.34E+08	4.51E+08	7.85E+08	2.81E+09	5.94E+07	2.87E+09
Ravine (m²)	0.00E+00	1.64E+06	1.64E+06	6.02E+05	1.62E+06	2.22E+06	0.00E+00	1.28E+06	1.28E+06	5.14E+06	3.87E+06	9.01E+06
Bluff (m²)	8.62E+03	2.90E+05	2.98E+05	4.70E+04	1.61E+05	2.08E+05	6.06E+04	1.83E+05	2.43E+05	7.50E+05	3.77E+05	1.13E+06
Stream length (m)	1.69E+05	4.56E+04	2.15E+05	1.82E+05	3.66E+04	2.19E+05	3.72E+04	1.37E+05	1.74E+05	6.08E+05	3.06E+04	6.38E+05

Annual suspended sediment loads measured at the 7 gages on the main branches of the Le Sueur, Cobb, and Maple rivers exhibit high variability between locations and from year to year for any given location as shown in Table 3.

Table 3 Annual sediment loads computed for each gaging station.

Basin	Contributing Drainage Area (km²)	TSS Load (Mg/yr)							
		2001	2002	2003	2004	2005	2006	2007	2008
Upper Maple	800	--	--	--	--	--	7,900	13,300	6,100
Lower Maple	880	--	--	18,607	101,200	85,100	22,300	37,900	22,300
Upper Cobb	335	--	--	--	7,500	8,200	4,000	4,400	3,100
Lower Cobb	735	--	--	--	--	--	33,400	21,800	14,600
Upper Le Sueur	870	--	--	--	--	--	--	42,200	22,400
Mid Le Sueur	1210	--	--	--	--	--	86,600	74,600	42,800
Mouth Le Sueur	2880	346,500	90,200	71,100	338,000	219,300	135,400	136,400	86,300

Aerial photo analysis of bluff retreat on the Maple River gives a range of bluff crest retreat rates between 0 – 0.67 m/yr. The mean retreat rate is 0.15 ± 0.07 m/yr. Extrapolating this average retreat rate to the 122 bluffs found throughout the Maple River yields a total of 31,700 ± 10,300 m³/yr assuming wedge erosion and 63,400 ± 20,600 m³/yr assuming parallel retreat. This suggests that, after adjusting for bulk density and the proportion of sediment that likely travels as washload (0.65), as much as 37,100 to 74,200 ± 24,000 Mg of sediment could be contributed from bluffs. By these estimates, 4,100 to 8,200 Mg would be contributed from bluffs located above the upper Maple gaging station, 15,600 to 31,200 Mg would be contributed between the upper and lower gages, and the remaining 17,400 to 34,800 Mg would be contributed below the lower gage. Results from interannual comparisons of bluff erosion using ground-based lidar are reasonably consistent with the rates observed from air photo analysis with a mean of 0.13 m/yr.

Planform changes in ravine morphology were not detectable in our analysis comparing 1938 and 2005 aerial photographs. In a few locations ravine tips grew slightly, and in other locations ravine tips were filled in. However, air photos do not likely have adequate resolution to identify ravine widening, nor do they have the ability to inform our understanding of ravine incision. Sediment gaging in the Hwy90 (including the upper and lower site) and Hwy8 ravines indicate

relatively small loads during 2008. Including storms for which we extrapolated TSS concentrations (as a function of flow) the loads were 11.5 – 17 Mg at UHwy90, 107 – 130 Mg at LHwy90, and 299 – 412 Mg at Hwy8. The numerical model simulating ravine erosion (Azmera et al., 2009) estimated that average annual sediment loads from the ravines are 140 Mg and 160 Mg for Hwy90 and Hwy8, respectively, 95% of which is derived from within the ravine itself, with the remainder derived from the uplands surrounding the ravine. Normalizing for the area of the ravine, this indicates a ravine sediment yield between 4 and 12 Mg/ha/yr. The UHwy90 site could be used as a constraint on upland contribution because there is little opportunity for sediment input from the ravine itself upstream from that point, so most of the sediment is likely derived from the uplands. The upland yield calculated from the 2008 load is 5.1 Mg/km^2/yr, which is considerably lower than other estimates for upland yield. In part this may be because 2008 was a particularly dry year and in part this may be because all of the tile drainage in the UHwy90 ravine watershed is subsurface drainage, with no surface inlets.

Net local streambank contributions that result from the process of meander migration were computed as a function of meander migration rate and the difference in elevation between the banks ($\Delta\eta$), as extracted from lidar for the Maple River. Table 4 shows the average $\Delta\eta$ extracted from lidar for the Maple River above and between the gaging stations in addition to the net sediment contribution in terms of volume, total mass, washload mass, and normalized per river kilometer.

Table 4 Net local sediment contributions from banks in the Maple River.

	Mean $\Delta\eta$	Net volume of sediment (m^3/yr)	Net mass of sediment (Mg/yr)	Net mass of washload (Mg/yr)	Mass of washload per river km (Mg/km/yr)
Above upper Maple gage	0.7	4500	5850	2900	67
Between Maple gages	1.1	1700	2210	1100	31

If one assumes that 100% of the sediment measured at the upper gages is derived from uplands the upper gage loads can be used to compute yield. The results are relatively consistent for the Maple and Cobb, but the Le Sueur exhibits significantly higher yield, as shown in Table 5. Taking these yields and applying them to the drainage area between the gages provides an estimate of the proportion of sediment contributed between the gages that is derived from uplands. In the Maple, Cobb, and Le Sueur that estimate is 27%, 28%, and 52%, respectively, but the uncertainty associated with this estimate is difficult to assess. This estimate could be considered an upper bound, because the yields computed from the upper gages were clearly upper bounds. However, the uplands between the gages tend to be more directly connected to the river, suggesting that the yields may actually be higher.

Table 5 Maximum constraints on upland sediment yields in the upper basins.

Basin	Upstream Area (km^2)	Sediment Yields (Mg/km^2)		
		2006	2007	2008
Upper Maple	800	9.9	16.6	7.6
Upper Cobb	335	11.9	13.1	9.3
Upper Le Sueur	870	--	48.5	25.7
UHwy90 Ravine	2.25	--	--	5.1

A long term record of net sediment deposition is preserved in the more than 400 strath erraces that we have mapped in the knickzone of the Le Sueur, Cobb, and Maple rivers (Gran et al., 2009). Taking the area between the upper and lower Maple River gages (1.15E+7 m^2) and subtracting active floodplain (4.5E+6 m^2) the annual rate of sediment storage in terraces has been approximately 1500 Mg/yr, averaged over the 12,000 years that the river has been incising. Terrace grain size distributions are similar to modern floodplains in grain size distribution, approximately 50% of which we estimate would be transported as washload. This yields a net deposition rate of fine sediment throughout the Holocene of 20 Mg per river km per year. Whereas this coarse estimate of long term deposition rates in the knickzone may or may not be indicative of current rates, which are driven by the anthropogenically altered hydrology and sediment dynamics, the natural feedback mechanisms built into channel-floodplain exchange suggest that this is a reasonable order of magnitude estimation with which modern measurements could be compared. During the 2009 field season one event inundated floodplains in the upper Maple River and sediment deposition was documented to range between 0 – 6 cm. More observations are needed to develop a reasonable empirical relationship between inundation, sediment concentration, and floodplain deposition.

The full utility of the sediment routing model cannot be realized until uncertainties in the sediment budget are reduced. Specifically, uncertainties need to be reduced in floodplain deposition above and within the knickzone, as well as bluff erosion rates and an upper bound for ravine sediment loads. However, baseline runs have been conducted that demonstrate that the model is stable for short (decadal) as well as long (millennial) term simulations. The model has successfully been run to steady-state conditions and the concentration and distribution of radionuclide tracers agrees with the analytical solution described in Lauer and Willenbring (in review). Results from a 6,000 year run illustrate the sensitivity of the model to knickpoint propagation, meander migration (0.1 m/yr above the knick, 2 m/yr below the knick), and exchange of sediment and tracers between the channel and floodplain (Figure 3).
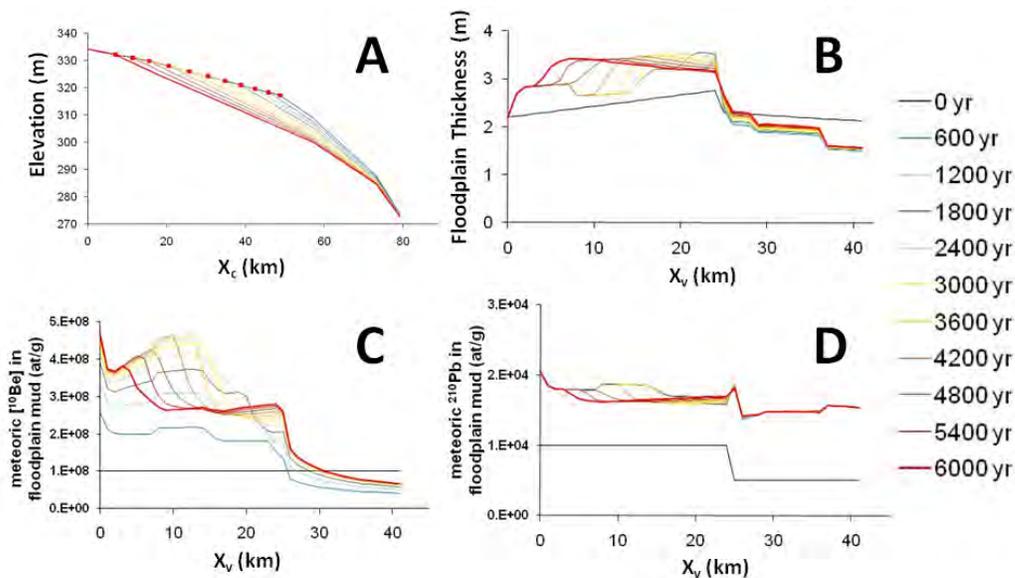

Figure 3 Results from a 6,000 year simulation illustrating reasonable and interpretable morphodynamic evolution of the channel profile (A) and floodplains (B) as well as sensitivity to the concentration and distribution of radioactive tracers ([10]Be and ^{210}Pb in C and D, respectively) in floodplain mud.

DISCUSSION

A sediment budget is a simple accounting tool that provides the basis for comparing all available information to assess the relative importance of the various sources and sinks throughout the watershed. It is built using empirical data and is therefore tied to the timeframe over which data is collected as well as the rigor of the various methods by which it is collected. Error associated with each method can and should be accounted for, but it is not always entirely straightforward how to propagate errors in a meaningful way in the context of a large watershed sediment budget. The relevance and inherent uncertainty of a sediment budget is also directly linked to the variability of the environmental parameters over time. Therefore it may or may not necessarily be a valid predictor for conditions where any of the measured variables fall outside the range observed during development of the budget (e.g. extremely wet or dry years).

One of the hard constraints against which the sediment budget must be tested is the sediment gaging data. These data provide critical information about sediment loads at different locations throughout the watershed, but do not necessarily provide information about relative importance of the different sediment sources. In the case of the Le Sueur, where the gages have been strategically placed above and below the knickpoint, the gaging data show that the majority of the sediment is introduced within the knickzone (Table 3) where the vast majority of the bluffs and ravines are located. However, the uplands are more directly linked to the fluvial network in the knickzone. Also, the difference in bank heights, and therefore net bank contributions according to Equation 1, is likely to be higher because vertical incision continually lowers the channel as the channel sweeps laterally back and forth across the valley bottom. So it should be expected that all four of the sources increase sediment yield in the knickzone. Folle (2010) estimates 13-30% of the annual suspended sediment load observed at the mouth of the Le Sueur originates from agricultural fields, with the remainder derived from bluffs, ravines, and streambanks.

Bluff erosion rates measured as part of this study from aerial photographs and ground-based lidar converge on retreat rates on the order of 0.15 m/yr with significant variability from bluff to bluff. The air photo analysis and ground-based lidar analysis translate to unit erosion rates of 0.085 (N = 121) and 0.084 Mg/m^2/yr (N = 8), respectively. These estimates are both slightly lower, but within the range of variability of results from a field survey conducted by Sekely et al. (2002), who measured annual volumes of sediment eroded from seven bluffs on the Blue Earth River, which translate to unit erosion rates of 0.176 Mg/m^2/yr, when properly adjusted for bulk density of 1.8 Mg/m^3 and 65% fines.

From our limited sampling, ravines appear to be responsible for a relatively small, but non-negligible amount of sediment within the knickzone. This is consistent with the estimate that ravines make up only on the order of 10% of the sediment excavated from the knickzone over the Holocene (Gran et al., 2009). The yields computed here fall within the wide range of yields reported for ephemeral gullies by Poesen et al. (2003), however it should be noted that ravines in the Le Sueur are significantly larger and more complex than those discussed by Poesen et al. (2003). Because we have only had the opportunity to monitor the ravines during dry years, at this time we are unable to put an upper constraint on sediment yields from these features in wet years. Furthermore, we have observed systematic changes in ravine morphology with distance along the river. Specifically, ravines tend to be the largest, steepest, and most incised near the

mouth of the river and smaller, less steep, and less incised higher up in the system. The ravines we monitored were in the middle of the knickzone and therefore might be considered average in some respects, but we recognize that erosional processes often exhibit non-linearities and simply applying the area-normalized yield from our monitored ravines to all other ravines may introduce a systematic bias that may be difficult to account for without monitoring other ravines both up- and downstream.

The banks of the stream channel can serve as net sources or sinks for sediment. During the process of meander migration banks deposit on one side of the channel and erode on the other side. In meandering channels, banks are typically net sources of sediment locally by virtue of the fact that the eroding bank is typically higher in elevation than the depositing bank (Lauer and Parker, 2008). The term local is used here because the contribution of sediment from a bank at the scale of a meander bend may be in part, or wholly, offset by net deposition on the floodplain at the reach scale. Table 4 above shows the net local contribution of sediment from banks as a result of meander migration. This estimate does not include the net source of sediment from banks as a result of channel widening. For an average channel depth of 2 m, a widening rate of 0.05 m, a bulk density of 1.3 Mg/m^3 and assuming 50% of the total mass is transported as suspended load, widening would contribute an additional 65 Mg/km/yr, which sums to an additional 2800 Mg/yr contributed from the banks above the upper gage within Blue Earth County in the Maple River and an additional 2300 Mg/yr contributed between the Maple gages.

The sediment routing model provides critical insight into the sediment dynamics of the system and has been developed to function in combination with the sediment budgeting analysis. Specifically, the routing model provides the opportunity to make predictions about morphological changes that result from alterations in hydrology and sediment transport in the system, the abundance and distribution of geochemical tracers, and the lag times associated with changes in management (i.e. when will reductions in one part of the watershed result in morphological or geochemical changes downstream?). Although some of the input parameters are still preliminary, the model is yielding important and interpretable results. Figure 3A shows the progression of the knickpoint with incision modeled as rigid rotation around a fixed point at the mouth of the river. Figure 3B illustrates the morphological changes in floodplain thickness; floodplains initially grow in thickness as the knickpoint passes (as a result of incision), and deflate over time as the river reworks the valley bottom. Figure 3C shows an initial increase in meteoric [10]Be concentration with a dramatic transition in the wake of the knickpoint, and trend toward an equilibrium concentration as a result of floodplain replacement from lateral meander migration. Figure 3D illustrates a less dramatic transition in the wake of the knickpoint for the ^{210}Pb tracer, which quickly reaches an equilibrium profile because of its short half life (22.3 years compared to 1.4E+6 years for [10]Be).

The combination of field observations, remote sensing analysis, geochemical fingerprinting, and modeling indicate that the relative magnitude of different sources, from largest to smallest as observed at the mouth of the Le Sueur appears to be bluffs, uplands, ravines, and the combined channel-floodplain system. However, work ongoing through the 2010 sampling season will continue to reduce uncertainty and better constrain natural variability of sediment sources and sinks throughout the watershed. Additional [10]Be and ^{210}Pb sediment fingerprinting analyses will be targeted at documenting the temporal variability of source inputs over the course of individual

events. Ongoing analyses combining the sediment budget and routing model, especially simulating pre-agricultural conditions as well as future alternative management scenarios, will provide the basis for identifying optimal locations for watershed rehabilitation and generating reasonable expectations for the timing and magnitude of load reductions.

REFERENCES

Azmera, L., Miralles-Wilhelm, F., Garcia, R., Belmont, P., and Melesse A. (2009) Modeling of ravine sediment loading and budget in the lower Le Sueur River, Minnesota River Watershed. AGU Fall Meeting, San Franciso, CA. Dec. 14-18, 2009.

Blann, K. L., Anderson, J. L., Sands, G. R. and Vondracek, B. (2009) Effects of Agricultural Drainage on Aquatic Ecosystems: A Review. Critical Reviews in Environmental Science and Technology, 39: 11, 909 - 1001.

Changnon, S.A., Kunkel, K.E., 1995. Climate-related fluctuations in midwestern floods during 1921–1985. Journal of Water Resources Planning and Management 121 (4), 326–334.

Clayton, L., and Moran, S.R., (1982) Chronology of late-Wisconsinan glaciations in middle North America: Quaternary Science Reviews, v. 1, p. 55–82.

Engstrom, D.R., Almendinger, J.E., and Wolin, J.A., (2009) Historical changes in sediment and phosphorus loading to the Upper Mississippi River: Mass-balance reconstructions from the sediments of Lake Pepin. Journal of Paleolimnology. 41: 563 – 588.

Folle, S.M. (2010) SWAT Modeling of sediment, nutrients, and pesticides in the Le Sueur River Watershed, south-central Minnesota. Ph.D. Dissertation, University of Minnesota.

Gran, K.B., Belmont, P., Day, S.S., Jennings, C., Johnson, A., Perg, L., and Wilcock, P.R., (2009) Geomorphic evolution of the Le Sueur River, Minnesota, USA, and implications for current sediment loading, *in* James, L.A., Rathburn, S.L., and Whittecar, G.R., eds., *Management and Restoration of Fluvial Systems with Broad Historical Changes and Human Impacts*: Geological Society of America Special Paper 451, p.119-130.

Johnson, S.L., Stefan, H.G., 2006. Indicators of climate warming in Minnesota: lake ice covers and snowmelt runoff. Climatic Change 75 (4), 421–453.

Kelley, D.W., and Nater, E.A., (2000) Historical sediment flux from three watersheds into Lake Pepin, Minnesota, USA: Journal of Environmental Quality, 29: 561–568.

Lauer, J.W., and Parker, G. (2008) Net local removal of floodplain sediment by river meander migration. Geomorphology. 96: 123–149.

Lauer, J.W., and Willenbring, J. (in review) Steady-state reach-scale theory for radioactive tracer concentration and sediment aging in a simple channel/floodplain system. in review JGR-ES.

Marschner, F.J., 1974, The original vegetation of Minnesota, a map compiled in 1930 by F.J. Marschner under the direction of M.L. Heinselman of the U.S. Forest Service: St. Paul, Minnesota, Cartography Lab of the Department of Geography, University of Minnesota.

Matsch, C.L., 1983, River Warren, the southern outlet of Lake Agassiz, *in* Teller, J.T., and Clayton, L., eds., Glacial Lake Agassiz: Geo. Assoc. of Canada Sp. Paper 26: 232–244.

Minnesota Department of Natural Resources (2007) Native Plant Communities and Rare Species of the Minnesota River Valley Counties: St. Paul, MDNR, Minnesota County Biological Survey Biological Report 89.

Minnesota Pollution Control Agency (MPCA), Minnesota Department of Agriculture, Minnesota State University, Mankato Water Resources Center, and Metropolitan Council Environmental Services, 2007, State of the Minnesota River: Summary of Surface Water Quality Monitoring, 2000–2005: St. Paul, 20 p.

Prince, H. (1997) Wetlands of the American Midwest. University of Chicago Press, Chicago, IL

Sekely, A.C., Mulla, D.J., and Bauer, D.W., (2002) Streambank slumping and its contribution to the phosphorus and suspended sediment loads of the Blue Earth River, Minnesota. J. of Soil and Water Cons. 57 (5): 243-250.

Spaling, H., and Smit, B. (1995). Conceptual model of cumulative environmental effects of agricultural land drainage. *Agr. Ecosyst. Environ.,* 53, 299–308.

Thompson, J. (2002). Wetlands drainage, river modification and sectoral conflict in the lower Illinois Valley, 1890–1930. Southern Illinois University Press, Carbondale, IL

Torri, D., Borselli, L. (2003) Equation for high-rate gully erosion. Catena 50, 449– 467.

Viparelli, E., Lauer, J.W., and Parker, G. (in prep A) Theory and problems related to equilibrium of a one reach morphodynamic sediment routing model. For JGR-Earth Surface.

Viparelli, E., Lauer, J.W., Parker, G., and Belmont, P. (in prep B) Application of a two reach morphodynamic sediment routing model to the Maple River, Minnesota. For JGR-ES.